Singlet ground states in compounds with a [MnIII 4 O2]8+ core due to broken degeneration†

Luis Escriche-Tur,[*ab] Belén Albela,[b] Mercè Font-Bardia[c] and Montserrat Corbella[*ad]

a Departament de Química Inorgànica i Orgànica (Secció inorgànica), Universitat de Barcelona, C/ Martı´ i Franque`s 1-11, 08028 Barcelona, Spain.
E-mail: luis.escrichetur@gmail.com , montse.corbella@qi.ub.es
b Laboratoire de Chimie, ENS de Lyon, Universite´ de Lyon, 46 Alle´e d'Italie, 69364 Lyon Cedex 07, France
c Cristal·lografia, Mineralogia i Dipo`sits Minerals, Universitat de Barcelona, Martı´ i Franque`s s/n, 08028 Barcelona, Spain
d Institud de Nanocie`ncia i Nanotecnologia de la Universitat de Barcelona (IN2UB), Av. Joan XXIII s/n, 08028 Barcelona, Spain

.

ABSTRACT:

Two new tetranuclear compounds with a formula [MnIII4 (m-O)2(m-4-RC6H4COO)7 m(L)2m(phen)2](ClO4)1+m, where R = MeO or tBu and m = 0 or 1, were synthesised and studied structurally and magnetically. The core of these compounds comprises a central Mn2O2 rhombus to which two terminal ions are attached – one to each oxo bridge. There are two types of bridges that alternately bind the central and terminal ions, those having a triple (m-O)(m-RCOO)2 or a double (m-O)(m-RCOO) bridge. The fit of the magnetic data of analogous compounds has so far been performed considering two different magnetic interactions, that between central ions (J1) and those between terminal and central ions (Jct), leading to ground states with ST = 2 or 3, or to five energetically degenerate ground states with ST = 0–4, depending on the J1/Jct ratio. In contrast, the compounds presented herein show an isolated ST = 0 ground state, and it was necessary to distinguish the two types of magnetic interactions between central and terminal ions (J2 and J3) to achieve a good fit of the experimental data. The differentiation of these interactions causes a spin state redistribution: the degeneration of ST = 0–4 breaks and the states with ST a 0 become unstable as J2 and J3 become more different. Nevertheless, the assignment of these states to a particular spin configuration was unachievable because the composition of these states changes upon decreasing the J3/J2 ratio. The importance of considering the relative orientation of Jahn–Teller axes is also highlighted.

INTRODUCTION

In the past few years many tetranuclear Mn compounds have been synthesised and characterised either to mimic the water oxidizing center1 or to study the ground-state spin frustration that is characteristic of these kinds of compounds.2,3 Moreover, such clusters possess large numbers of unpaired electrons, making them attractive as precursors for other magnetic materials.4 Some of the first compounds synthesised contained a [Mn4O2]6+/7+/8+ core, where the metals could be arranged either in a planar or a non-planar (‘‘butterfly’’) fashion (Fig. 1), and the Mn oxidation states are MnII 2MnIII 2 , MnIIMnIII 3 or MnIII 4 .2,3,5–17

The variability of the ground-state spin and the presence of spin frustration in these tetranuclear compounds have been profoundly studied for both MnIII 4 and mixed-valence compounds. The resulting ground state depends on the relative magnitude of the magnetic interactions between the central Mn ions (Jcc or J1) and those between central and terminal ions (Jct), both being antiferromagnetic. In particular, MnIII 4 compounds may display a ground state with ST = 2 or 3, or have five energetically degenerate ground states with ST = 0–4, depending on the J1/Jct ratio.

The analysis of the magnetic data for these compounds is rather challenging, since there are five Mn□ □ □ Mn interactions and the presence of MnIII ions may lead to substantial zero-field splitting (ZFS) that makes such properties more difficult to understand. In fact, among several examples found in the literature, the analyses were performed applying several approximations3,17 or without analysing the data completely, especially in the low temperature range.2,5,8

In this work we present the synthesis and crystal structures of two new [MnIII 4 O2]8+ compounds with a general formula [Mn4(m-O)2(m-4-RC6H4COO)7 m(L)2m(phen)2](ClO4)1+m, where R = MeO (1) or tBu (2) and m = 0 or 1. The crystal structure of compound 1 could be determined without any complication, as we obtained high-quality single-crystals. However, the crystals obtained for 2 were unfortunately poorly diffracting, and only the formula and approximate structural parameters of 2 could be obtained. We also report an in depth study of the magnetic properties and the influence of the relative magnitude of the Mnc□ □ □ Mnt interactions on the resulting spin state distribution. The inclusion of the axial anisotropy parameter (DMn) and the consideration of the relative disposition of the Jahn–Teller axes of the MnIII ions enabled us to completely fit the magnetic data and to estimate the approximate values of the ZFS of the MnIII ions.

.

EXPERIMENTAL SECTION

Synthesis

All manipulations were performed under aerobic conditions. Reagents and solvents were obtained from commercial sources and used without further purification. NBu4MnO4 was prepared as described in the literature.18 Caution! Perchlorate salts of compounds containing organic ligands are potentially explosive. Only small quantities of these compounds should be prepared.

[Mn4(l-O)2(l-4-MeOC6H4COO)7(phen)2]ClO4 (1). 4-MeOC6H4- COOH (2.89 mmol, 0.44 g) and Mn(ClO4)2 6H2O (1.32 mmol, 0.48 g) were dissolved in acetonitrile. Then, solid NBu4MnO4 (0.33 mmol, 0.12 g) was added to the previous solution in small portions for 1–2 min while, almost simultaneously, 10 mL acetonitrile solution of 1,10-phenanthroline (phen) (0.83 mmol, 0.16 g) was added, also in small portions. The resulting dark solution (total volume B20 mL) was stirred for 10 minutes and dried with a rotary evaporator. The resulting black oil was dissolved in a CH3CN: EtOH (10 : 10 mL) mixture and filtered to separate any possible residue. Dark red crystals were obtained after a week of slow evaporation at roomtemperature. Yield: 25%. Anal. calcd for C80H65ClMn4N4O27 (M.W. = 1769.59 g mol 1) (%): C, 54.30; H, 3.70; N, 3.17. Found (%): C, 53.67; H, 3.73; N, 3.17. Selected IR data (cm 1): IR (cm 1): 3446 (br), 3070 (w), 2931 (w), 2836 (w), 1602 (s), 1559 (s), 1507 (m), 1457 (w), 1420 (m), 1380 (s), 1359 (s), 1314 (m), 1256 (s), 1170 (s) 1086 (m), 1025 (m), 852 (w), 790 (m), 749 (w), 667 (w), 621 (m), 504 (w), 437 (w).

[Mn4(l-O)2(l-4-tBuC6H4COO)6(H2O)2(phen)2][Mn4(l-O)2(l-4-tBuC6H4COO)6(CH3CN)2(phen)2](ClO4)4 (2). 4-tBuC6H4COOH (1.75 mmol, 0.31 g) and Mn(ClO4)2 6H2O (0.8 mmol, 0.29 g) were dissolved in acetonitrile (10 mL). Then, solid NBu4MnO4 (0.20 mmol, 0.082 g) was added to the previous solution in small portions for 1–2 minutes while, almost simultaneously, an acetonitrile solution (10 mL) of 1,10-phenanthroline (phen) (0.50 mmol, 0.10 g) was added, also in small portions. Finally, solid NaClO4 H2O (10.6 mmol, 1.3 g) was added. The resulting dark red solution (total volumeB25 mL) was stirred for 15 min and shortly afterward filtered to separate any possible residue. After leaving the solution undisturbed for three weeks, dark red crystals were isolated by filtration, washed with ether and dried under vacuum. Single-crystals were obtained under the same conditions but using less NaClO4 H2O (9.8 mmol, 1.2 g). Yield: 16%. Anal. calcd for C92H99Cl2Mn4N5O23 (average formula, referred to one Mn4 unit) (M.W. = 1933.45 g mol 1) (%): C, 57.15; H, 5.16; N, 3.62. Found (%): C, 58.10; H, 5.32; N, 3.50. Selected IR data (cm 1): 3434 (br), 3075 (w), 2960 (m), 2906 (w), 2869 (w), 1597 (s), 1555 (s), 1521 (s), 1462 (w), 1383 (s), 1310 (w), 1269 (w), 1193 (w) 1101 (s), 1015 (w), 854 (m), 786 (m), 722 (m), 652 (m), 623 (m), 601 (m), 548 (w), 479 (m).

Physical characterisation

C, H and N analyses were carried out by the ‘‘Centres Cientı´fics i Tecnolo`gics’’ of the Universitat de Barcelona. Infrared spectra were recorded on KBr pellets in the 4000–400 cm 1 range using a Thermo Nicolet Avatar 330 FTIR spectrometer. Magnetic measurements were performed on microcrystalline samples in a Quantum Design MPMS XL5 SQUID Magnometer at the ‘‘Unitat de Mesures Magne`tiques’’ (Universitat de Barcelona). Magnetic susceptibility was measured between 2 and 300 K and with a magnetic field of 0.02 T. The fit of the experimental magnetic data was performed by minimizing the function R = P[(wMT)exp (wMT)calcd]2/P[(wMT)exp]2.

Single-crystal X-ray crystallography

The data collection for compounds 1 and 2 was performed on a Bruker Apex-II diffractometer at 100 K, equipped with a graphite monochromatic Mo Ka radiation (l = 0.71073 Å). Unit-cell parameters were determined from B9500 reflections and refined by the least-squares method. Several thousand reflections (161 200 for 1 and 84 790 for 2) were collected using the F- and o-scan. Data were corrected for absorption effects using the multi-scan method (SADABS).19 Table S1 (ESI†) contains the crystallographic data collection and structure refinement details. The structures were solved by direct methods and refined by full-matrix leastsquares using SHELXL-2016/6,20 run by the Wingx21,22 and ShelXle23 user interfaces, respectively. Non-hydrogen atoms were refined anisotropically, whereas hydrogen atoms were computed and refined with isotropic thermal parameters riding on their respective carbon or oxygen atoms. Particularly, solvent hydrogen atoms interacting with neighbours were placed in ideal positions.

Compound 1 1/2 EtOH 5/4 CH3CN 1/4H2O crystallises in triclinic space group P1. The asymmetric unit consists of two conformational isomers of the [Mn4(m-O)2(m-4-MeOC6H4COO)7(phen)2]+ complex, two perchlorate anions and some solvent molecules (H2O, CH3CN and EtOH). A total of 2240 parameters were refined in the final refinement on F2 using 75 restraints.

Single-crystals of compound 2 were isolated and mounted on the diffractometer. However, the crystals of this compound were very thin and gave highly poor statistics (Rint = 0.253). Then, the structure could not be completely refined and, therefore, it was not deposited in the CCDC database. Even so, the Q peaks could be assigned to all atoms and isotropically refined. This compound crystallises in the triclinic space group P21/c. The asymmetric unit consists of a half of the [Mn4(m-O)2(m-4-tBuC6H4COO)6(H2O)2(phen)2]2+ and of the [Mn4(m-O)2(m-4-tBuC6H4COO)6(CH3CN)2(phen)2]2+ complexes, two perchlorate anions, and two acetonitrile molecules. The whole complexes are generated by an inversion centre situated in the middle of them.

RESULTS AND DISCUSSION

Synthesis

Both tetranuclear compounds 1 and 2 were obtained from the reaction of comproportionation between MnII and MnO4 in the presence of a substituted derivative of benzoic acid and 1,10-phenanthroline (phen), leading to compounds with general formula [Mn4(m-O)2(m-4-RC6H4COO)7 m(L)2m(phen)2](ClO4)1+m, where R = MeO (1) or tBu (2), L is a monodentate ligand, and m = 0 or 1.

The mother liquors of 1 and 2 were left to slowly evaporate, but no solid was obtained from either of them, indicating that both compounds are highly soluble in acetonitrile. Thus, they needed to be crystallised by mixing the mother solution with absolute ethanol (1) or by adding a huge excess of ClO4 anions (2). For compound 1, crystallisation from different CH3CN: EtOH mixtures was tried, but no differences were observed changing the CH3CN/EtOH volume ratio (from 0.3 to 0.7). In all cases, the reaction yield was about 25% considering the stoichiometry of the reaction above. In contrast, we had some difficulties finding the optimum conditions to obtain compound 2 in appreciable yield. Its crystallisation needed to be assisted by the addition of about 22 equivalents of ClO4 anions, leading to 2 in 16% yield. If the amount of ClO4 anions used is decreased, crystallisation becomes very slow and ineffective. For instance, it took nearly three months to obtain only a couple of crystals of 2 using 11.5 equivalents of ClO4 .

Description of structures

The crystal structures of these compounds consist of two cationic complexes, perchlorate anions and molecules of solvent. Simplifications of these structures are represented in Fig. 2, respectively. Fig. S1 (ESI†) contains the fully labelled crystal structures of 1 and 2. The most relevant structural parameters are listed in Tables S2 and S3 (ESI†). It is worth remembering that the crystal structure of 2 could not be fully refined, and just approximate values of some structural parameters are provided.

Both compounds contain a [MnIII 4 (m3-O)2]8+ core comprising two central (Mnc) and two terminal (Mnt) ions. There is an Mnc2Ob2 rhombus to which the Mnt ions are attached – one to each m3-O2 ligand. The Mnc□ □ □ Mnc distances are B2.85 (1) or B2.88 (2) Å, and the Mnc–Ob–Mnc angles are in the 96–991 range. There are two types of bridges that alternately bind the Mnc and Mnt ions, those having a triple (m-O)(m-RCOO)2 or a double (m-O)(m-RCOO) bridge. The Mnc□ □ □ Mnt distances where Mn ions are linked by a triple bridge (B3.25–3.31 Å) are shorter than those of the double bridge (B3.35–3.41 Å). Similarly, the Mnc–Ob–Mnt angles corresponding to the triple bridges (B120–1261) are smaller than those corresponding to the double bridges (B126–1321). All these structural parameters are in accord with those of compounds with a [Mn4O2]6+/7+/8+ core and carboxylate bridges.2,3,5–17,24

In both crystal structures there are six carboxylate ligands linking Mnc with the Mnt ions. Four of these ligands are approximately in the same plane of the central Mnc2O2 rhombus, whereas the other ones are perpendicular to this rhombus. Furthermore, compound 1 has an additional carboxylate bridge that links the two Mnc ions. In contrast, these seventh positions in 2 are instead occupied by monodentate ligands that lie on the opposite sides of the Mnc2Ob2 rhombus. Then, while the cationic complexes of 2 display different monodentate ligands, one having two molecules of CH3CN and the second one of H2O, those of 1 are just conformational isomers.

The seventh carboxylate ligand in 1 causes some other differences in the structural parameters of the metallic core. For instance, while the Mnc2Ob2 rhombus is completely planar in 2, that of 1 is slightly twisted, with an Mnc–Ob–Ob–Mnc angle of B1681. Concerning the Mn4 arrangements, in 2 the four Mn ions are in the same plane, one of the Mnt ions being below the Mnc2Ob2 rhombus and the other one above. On the other hand, both Mnt ions in 1 are placed above the central rhombus, resulting in a butterfly-like arrangement (Fig. 1).

All Mn atoms in compounds 1 and 2 have an elongated pseudo-octahedral geometry, displaying Jahn–Teller distortion, as expected for MnIII ions. Jahn–Teller axes in Mnc ions are almost parallel, whereas they are nearly perpendicular to those of Mnt ions (Fig. 3). Considering the z axes in the direction of the Jahn–Teller axes and unfairly assigning the x and y axes, approximate values of lengths of the octahedron axes can be found with the addition of the Mn–ligand distances (see Table S4, ESI†). To quantify the distortions of the coordination octahedra, the procedure described in our previous work was followed,25 whose results are listed in Table S4 (ESI†). All Mn ions display an elongated distortion (z axes are longer than x and y axes) and an almost inappreciable rhombic distortion (x and y axes are very similar in length). The Mnc ions (with D = 10–18%) aremuchmore elongated than the Mnt ones (with D = 7.8–11%).

Magnetic properties

Magnetic susceptibility (wM) data were recorded for compounds 1 and 2 from 300 to 2 K. wMT versus T and wM versus T plots for 1 and 2 are shown in Fig. 4. Note that the molecular weight of 2 was referred to one Mn4 unit, considering an average formula between the two entities. The wMT value at room temperature is 8.3 cm3 mol K, which is quite below the expected value for four MnIII ions (12.0 cm3 mol K). wMT decreases with temperature almost linearly until B90 K and below this temperature it decreases drastically to B0.4 cm3 mol K at 2 K, indicating a strong antiferromagnetic behaviour. wM versus T plots for both compounds show nearly superimposable graphs between 300 and 80 K, but they differ below this temperature. While the wM versus T plot of compound 1 displays a maximum at 9 K (wM E 0.14 cm3 mol), the one of 2 is situated at 6 K (wM E 0.27 cm3 mol). This difference can also be seen in the wMT versus T plots. The presence of these maxima suggests that both compounds have a ground state with S = 0.

Four different Mn□ □ □ Mn exchange pathways may be considered (shown in Fig. 5): the magnetic interaction between the Mn ions bound with a double oxo bridge, J1 (Mnc□ □ □ Mnc); two centralterminal Mn ion interactions (Mnc□ □ □ Mnt), J2 and J3; and the magnetic interactions between terminal Mn ions, J4 (Mnt□ □ □ Mnt). The Heisenberg spin Hamiltonian (H) considered is

$$H = -2J_1(S_1S_2) - 2J_2(S_1S_3 + S_2S_4) - 2J_3(S_2S_3 + S_1S_4) - 2J_4(S_3S_4) \quad (1)$$

where S1 = S2 = S3 = S4 = 2. Several fits of the experimental data were performed, screening different values of the magnetic coupling constants (results shown in Fig. S2, ESI†). In all of them, the interaction between terminal Mn ions was considered negligible (J4 = 0). In fact, this interaction, with a Mn□ □ □ Mn distance of B5.6 Å, is expected to be of comparable magnitude to intermolecular interactions. Firstly, the experimental data were fitted considering J2 = J3 to get an average value of the central-terminal interactions, as usually performed for this kind of compound with a [Mn4O2]m+ core (m = 6–8);3,5,8,17,24,26 but the shape of the curve could not be reproduced with any of these fits. The inclusion of the DMn parameter, but still keeping J2 = J3, did not provide better fits. Therefore, the fits were performed considering J2 a J3, which gave more appropriate reproductions of the experimental curves. However, the shape of the maxima in the wM versus T plots was not completely reproduced in these latter fits indicating that the inclusion of ZFS parameters could provide better results. Indeed, considering that DMn improved the fits of the experimental data substantially the entire curves were reproduced much better. The rhombic zero-field splitting parameter was considered negligible (EMn = 0), in accord with the low rhombic distortion of the MnIII ions of these compounds (ro2%, see Table S4, ESI†). The relative orientation of the Jahn–Teller axes is an important factor that should be taken into account when the axial anisotropy of the Mn ions is appreciable. Indeed, we previously reported that this parameter may have an effect on the overall magnetic properties,25 especially in the low temperature range. In the tetranuclear compounds herein described, the Jahn–Teller axes are almost parallel between the central Mn ions and nearly orthogonal between the central and terminal ions (Fig. 3).
Hence, the experimental data were fitted (300–2 K) using the PHI program27 and taking into account the axial zero-field splitting (DMn) and the relative orientation of the Jahn–Teller axes of the MnIII ions. The best fits correspond to g = 2.01, 2J1 = 45.5 cm 1, 2J2 = 15.1 cm 1, 2J3 = 4.4 cm 1, and DMn = 3.5 cm 1 with R = 7.9 □ 10 5 for 1; and to g = 2.01, 2 J1 = 43.0 cm 1, 2J2 = 14.7 cm 1, 2J3 = 8.2 cm 1, and DMn = 3.6 cm 1 with R = 6.1 □ 10 5 for 2. The DMn values are consistent with elongated MnIII ions, which is expected to show moderate and negative DMn.28–31 Even though the ground states of these compounds have S = 0, the zero-field splitting of the first excited states may be of importance for the wM versus T plot when these states are populated at low temperature, as we reported previously.25 Accordingly, the energy level distribution calculated for these compounds with the parameters obtained from the fits (omitting DMn) revealed that the ground states have S = 0 and that there are several low-lying excited states with S a 0 (see below).

The strongest magnetic coupling constant (J1) is unambiguously assigned to the double-oxo bridge, since a strong antiferromagnetic interaction is expected for this subunit and it is consistent with that observed in analogous compounds (Table S5, ESI†). The assignment of J2 and J3 to the triple (m-O)(m-RCOO)2 or double (m-O)(m-RCOO) bridges appears much more challenging; for analogous systems they are indeed considered too similar to be differentiated, obtaining just an average value. However, its distinction was necessary in order to achieve a good fit of the experimental data for 1 and 2 (Fig. S3, ESI†). Aiming to their assignment, we compared the structural parameters of these subunits and dinuclear MnIII compounds with (m-O)- (m-R0COO) or (m-O)(m-R0COO)2 bridges. Only two examples of dinuclear MnIII compounds with a double (m-O)(m-R0COO) bridge were found, in which the magnetic coupling constants are quite different (2J = 19.5 and +1.33 cm 1 for H = 2JS1S2).32,33 However, both compounds display compressed MnIII octahedral (D E 10%, r E 1.5–6%), contrary to 1 and 2, making them non-comparable. The magnetic properties of dinuclear MnIII compounds with a triple (m-O)(m-R0COO)2 bridge have been extensively studied in our precedent study.25 The value of the magnetic interaction of this triple-bridged subunit may be approximately predicted using the magneto-structural correlation presented therein. However, these subunits in compounds 1 and 2, with D E 7.8–18% and r o 4%, are very different from those in the dinuclear MnIII compounds, which always show a significant degree of rhombicity (r = 3.5–5.4%). Hence, the assignment of these bridging blocks to certain values is very risky. We also tried to assign J2 and J3 by comparing the structural parameters of other compounds with a [MnIII 4 O2]8+ core and carboxylate bridges (Tables S6 and S7, ESI†), but no clear assignment could be done.

Spin states distribution

The magnetic properties of compounds with a similar structure to those of 1 and 2 were reported in the literature.3,5,6,17,24 As commented above, J2 and J3 were not distinguished and an average value of the Mnt Mnc interaction (Jct) was provided. These compounds usually show different spin ground states depending on the J1/Jct ratio. The most common ground state is (ST, Scc, Stt) = (3, 1, 4) for J1/Jct = 2.5–4.9.3,6,8,17 When J1/Jct44.9, then five energetically degenerate states, (n, 0, n) with n = 0–4, become the ground state,5,9,24 corresponding to two noninteracting Mnt ions.3 In the lower limit, when J1/Jct o 2.5 the ground state would be (2, 2, 4). In contrast, the compounds (1 and 2) presented herein display an isolated (0, 0, 0) ground state. The explanation of this fact lies in the differentiation of the two types of interactions between the terminal and central ions, J2 and J3 (following the diagram shown in Fig. 5). It is important to remember that there are two different Mnc Mnt magnetic interaction pathways: those consisting of a double (m-O)(m-R0COO) bridge and those having a triple (m-O)(m-R0COO)2 bridge. Fig. 6 shows energy of the first spin states versus J3/J2 plots for hypothetical compounds with a [MnIII 4 O2]8+ core, all energies being referred to the lower ST = 0 state. When J3 and J2 are equal (J3/J2 = 1), the spin ground state has ST = 3 and there are several states with ST = 0–4 that are energetically degenerated.

However, this degeneration breaks and all states increase in energy as the J3/J2 ratio decreases. For J3/J2 values between B0.6–0.7, the lowest spin states will be mixed and spin frustration is then plausible. When J3/J2 is below 0.6, the spin ground state is ST = 0. Then, compounds 1 and 2, with respective J3/J2 ratios of B0.3 andB0.6, have an ST = 0 ground state. Having this ground state is a key point for the distinction between J2 and J3. Indeed, if the J3/J2 ratio was 40.8, the corresponding system would display an ST = 3 ground state and wMT values would not approach zero at low temperature, as similarly observed when J3 = J2. Then, the distinction between these two magnetic interactions would be highly likely unachievable.

The separation between the ground and first excited states in these compounds is rather different: for 2 the three first excited states (with ST = 1, 2, and 3) are at the most at 10 cm 1 above the ground state, whereas they are much more separated for 1 (at 3.5–27 cm 1 above the ground state). As J1 and J2 values are very similar for both compounds, the cause of these different separations must rely on J3, the value of that of 2 is twice the one of 1. This difference is also responsible for the different degree of interaction observed in the wMT versus T and wM versus T plots, where the stronger interaction of 1 is confirmed. Nonetheless, it is surprising that the compound showing a smaller |J3| value has a stronger interaction. This fact can be also explained with the energy distribution of the excited states: the ST = 0 ground state in 1 is far more isolated than that in 2, maximizing the decrease of the wMT values upon cooling.

A deeper analysis of the energy levels as a function of the J3/J2 ratio may provide useful information concerning the spin configuration of the states. However, a non-intuitive and complex result was obtained from this analysis. Each one of these states, commonly named eigenstates, is the result of the combination of several configurations of single-ion spin moments. These configurations are known as basic elements. Moreover, the composition of these eigenstates changes upon decreasing the J3/J2 ratio. Then, the assignment of the states to a particular configuration is unachievable. As an example, Fig. 6 also shows the percentage composition (calculated with the PHI27 program) of the three most relevant (ST, Scc, Stt) basic elements in which the Hamiltonian is constructed for the ST = 0 and ST = 3 eigenstates that are lowest in energy. These eigenstates were not chosen arbitrarily, since the most common ground states are those having ST = 3 (for J3/J2 4 0.7) and ST = 0 (for J3/J2 o 0.6) according to the diagram of energy shown in Fig. 6. The spin configurations that represent these basic elements are represented in Fig. 7.

As may be observed, when J3/J2 = 1, the ST = 0 and the ST = 3 states mainly correspond to spin configurations with (ST, Scc, Stt) = (0, 0, 0) and (3, 1, 4), respectively, with contributions of at least B80%. However, the composition of these states changes upon decreasing the J3/J2 ratio and the assignment to a single spin configuration becomes unachievable. This fact is also observed for the rest of the eigenstates included in Fig. 6 except for the ST = 4 state, whose highest contribution is never lower than 70% and corresponds to the (4, 0, 4) configuration.

CONCLUSIONS

The reaction between Mn(ClO4)2 and Bu4NMnO4 in the presence of benzoic acid derivatives 4-MeOC6H4COOH (1) or 4-tBuC6H4- COOH (2) and 1,10-phenantroline (phen) led to the formation of two new tetranuclear compounds with a [MnIII 4 O2]8+ core, which comprises a central Mn2O2 rhombus to which two terminal Mn ions are attached – one to each m3-O2 ligand. The crystal structures of these compounds revealed that the Mn ions are arranged in a butterfly (1) or in a Mn4 planar (2) fashion. There are two types of magnetic interactions between central and terminal ions: those consisting of a double (m-O)(m-R0COO) bridge and those having a triple (m-O)(m-R0COO)2 bridge. The MnIII ions in these compounds display a significant elongated distortion along the Jahn–Teller axes and a negligible rhombic distortion. Moreover, the Jahn–Teller axes in the central Mn ions are almost parallel, while they are nearly perpendicular to those of the terminal Mn ions.

The magnetic measurements revealed that these compounds show an ST = 0 ground state. There are three different magnetic interaction pathways: one between central ions (J1) and two between central and terminal ions (J2 and J3). The distinction between J2 and J3 was crucial to obtain a good fit of the experimental data. However, the assignment of J2 and J3 to a particular bridging block was not achieved. The inclusion of the axial anisotropy parameter (DMn) and the consideration of the relative orientation of the Jahn–Teller axes led tomuch better fits. A deep analysis of the energy levels as a function of the J3/J2 ratio (from 1.0 to 0.0) provided very useful information. The distribution of energy levels changes completely with the J3/J2 ratio, having an ST = 0 ground state when J3/J2o0.6. Nevertheless, the assignment of the states to a particular configuration was unachievable because the composition of these states changes upon decreasing the J3/J2 ratio.

ACKNOWLEDGEMENTS

This work was supported by the Ministerio de Ciencia e Innovacio´n of Spain (project CTQ2012-30662 and CTQ2015-63614-P). L. E. thanks the University of Barcelona for the APIF fellowship.

REFERENCES

1 S.Mukhopadhyay, S.K.Mandal, S. Bhaduri andW. H. Armstrong, Chem. Rev., 2004, 104, 3981–4026.

2 B. Albela, M. S. El Fallah, J. Ribas, K. Folting, G. Christou and D. N. Hendrickson, Inorg. Chem., 2001, 40, 1037–1044.

3 J. B. Vincent, C. Christmas, H. R. Chang, Q. Li, P. D. W. Boyd, J. C. Huffman, D. N. Hendrickson and G. Christou, J. Am. Chem. Soc., 1989, 111, 2086–2097.

4 G. Christou, D. Gatteschi, D. N. Hendrickson and R. Sessoli, MRS Bull., 2000, 25, 66–71.

5 C. Can˜ada-Vilalta, J. C. Huffman and G. Christou, Polyhedron, 2001, 20, 1785–1793.

6 M. J. Knapp, D. N. Hendrickson, V. A. Grillo, J. C. Bollinger and G. Christou, Angew. Chem., Int. Ed. Engl., 1996, 35, 1818–1820.

7 Z. Chen, Y. Ma, F. Liang and Z. Zhou, J. Organomet. Chem., 2008, 693, 646–654.

8 Y.-S. Ma, H.-C. Yao, W.-J. Hua, S.-H. Li, Y.-Z. Li and L.-M. Zheng, Inorg. Chim. Acta, 2007, 360, 1645–1650.

9 T. Taguchi, M. R. Daniels, K. A. Abboud and G. Christou, Inorg. Chem., 2009, 48, 9325–9335.

10 R. Ruiz, C. Sangregorio, A. Caneschi, P. Rossi, A. B. Gaspar, J. A. Real and M. C. Mun˜oz, Inorg. Chem. Commun., 2000, 3, 361–367.

11 J. Pistilli andR. H. Beer, Inorg. Chem. Commun., 2002, 5, 206–210. 12 T. Tamane, T. Tsubomura and K. Sakai, Acta Crystallogr., Sect. C: Cryst. Struct. Commun., 1996, 52, 777–779.

13 S. Wang, M. S. Wemple, J. Yoo, K. Folting, J. C. Huffman, K. S. Hagen, D. N. Hendrickson and G. Christou, Inorg. Chem., 2000, 39, 1501–1513.

14 G. Aromı´, S. Bhaduri, P. Artu´s, K. Folting and G. Christou, Inorg. Chem., 2002, 41, 805–817.

15 N. E. Chakov, L. N. Zakharov, A. L. Rheingold, K. A. Abboud and G. Christou, Inorg. Chem., 2005, 44, 4555–4567.

16 M. Hołyn´ska and S. Dehnen, Z. Kristallogr. - Cryst. Mater. 2011, 226, 769–772.

17 E. Libby, J. K. McCusker, E. A. Schmitt, K. Folting, D. N. Hendrickson and G. Christou, Inorg. Chem., 1991, 30, 3486–3495.

18 T. Sala and M. V. Sargent, J. Chem. Soc., Chem. Commun., 1978, 253–254.

19 Bruker, SADABS, version 2008/1, Bruker AXS Inc., Madison, Wisconsin, USA, 2008.

20 G. M. Sheldrick, Acta Crystallogr., Sect. C: Struct. Chem., 2015, 71, 3–8.

21 L. J. Farrugia, J. Appl. Crystallogr., 1999, 32, 837–838.

22 L. J. Farrugia, J. Appl. Crystallogr., 2012, 45, 849–854.

23 C. B. Hu¨bschle, G. M. Sheldrick and B. Dittrich, J. Appl. Crystallogr., 2011, 44, 1281–1284.

24 G. Aromı´, S. Bhaduri, P. Artu´s, J.C.Huffman,D. N. Hendrickson and G. Christou, Polyhedron, 2002, 21, 1779–1786.

25 L. Escriche-Tur, M. Font-Bardia, B. Albela and M. Corbella, Dalton Trans., 2016, 45, 11753–11764.

26 U. Bossek, H. Hummel, T. Weyhermu¨ller, K. Wieghardt, S. Russell, L. van der Wolf and U. Kolb, Angew. Chem., Int. Ed. Engl., 1996, 35, 1552–1554.

27 N. F. Chilton, R. P. Anderson, L. D. Turner, A. Soncini and K. S. Murray, J. Comput. Chem., 2013, 34, 1164–1175.

28 R. Bocˇa, Coord. Chem. Rev., 2004, 248, 757–815. 29 S. Gomez-Coca, E. Cremades, N. Aliaga-Alcalde and E. Ruiz, J. Am. Chem. Soc., 2013, 135, 7010–7018.

30 C. Duboc, D. Ganyushin, K. Sivalingam, M.-N. Collomb and F. Neese, J. Phys. Chem. A, 2010, 114, 10750–10758.

31 G. Aromı´, J. Telser, A. Ozarowski, L.-C. Brunel, H.-M. Stoeckli-Evans and J. Krzystek, Inorg. Chem., 2005, 44, 187–196.

32 K. J. Oberhausen, R. J. O'Brien, J. F. Richardson, R. M. Buchanan, R. Costa, J. M. Latour, H. L. Tsai and D. N. Hendrickson, Inorg. Chem., 1993, 32, 4561–4565.

33 N. Arulsamy, J. Glerup, A. Hazell, D. J. Hodgson, C. J. McKenzie and H. Toftlund, Inorg. Chem., 1994, 33, 3023–3025.

Legends to figures

Figure. 1 Schematic representation of two arrangements for the [Mn4(m3-O)2] core. Label code: Mnc = central Mn ion, Mnt = terminal Mn ion, and
Ob = bridging oxygen atom.

Figure. 2 Crystal structures of the cationic complexes of 1 (only one of the subunits) and 2. The 4-RC6H4COO groups have been omitted for better clarity. Colour code: MnIII, brown; C, grey; N, blue; O, red.

Figure. 3 Schematic representation of the cationic complexes of 1 and 2. Green bold lines correspond to the Jahn–Teller axes. L could be H2O or CH3CN.

Figure. 4 wMT versus T and wM versus T (inset) plots for compounds 1 (red) and 2 (blue). The solid lines correspond to the best fit to the experimental data. The molecular weight of 2 was referred to one Mn4 unit, considering an average formula between the two entities

Figure 5. Schematic representation of the possible Mn Mn exchange pathways in compounds 1 and 2.

Figure 6 (a) Energy at zero field for the first spin states as a function of J3/J2 ratio for a hypothetical [MnIII 4O2]8+ compound with 2J1 = 45.6 cm 1, J2 = 15 cm 1, DMn = 0, and variable J3 values. The coloured lines correspond to the most relevant states. (b) Percentage composition of the three most relevant (ST, Scc, Stt) basic element in which the Hamiltonian is contracted for the eigenstates with ST = 0 and ST = 3 that are lowest in energy. J3/J2E0.3 for 1 and 0.6 for 2.

Figure 7 Possible spin configuration representing the most relevant (ST, Scc, Stt) spin states that configure the two lowest eigenstates with ST = 0 and ST = 3.

FIGURE 1

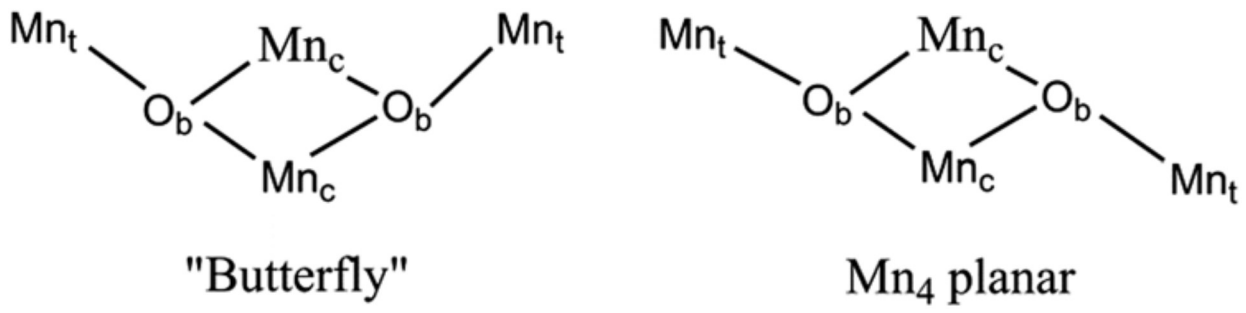

"Butterfly" Mn_4 planar

454 **FIGURE 2**

455

456

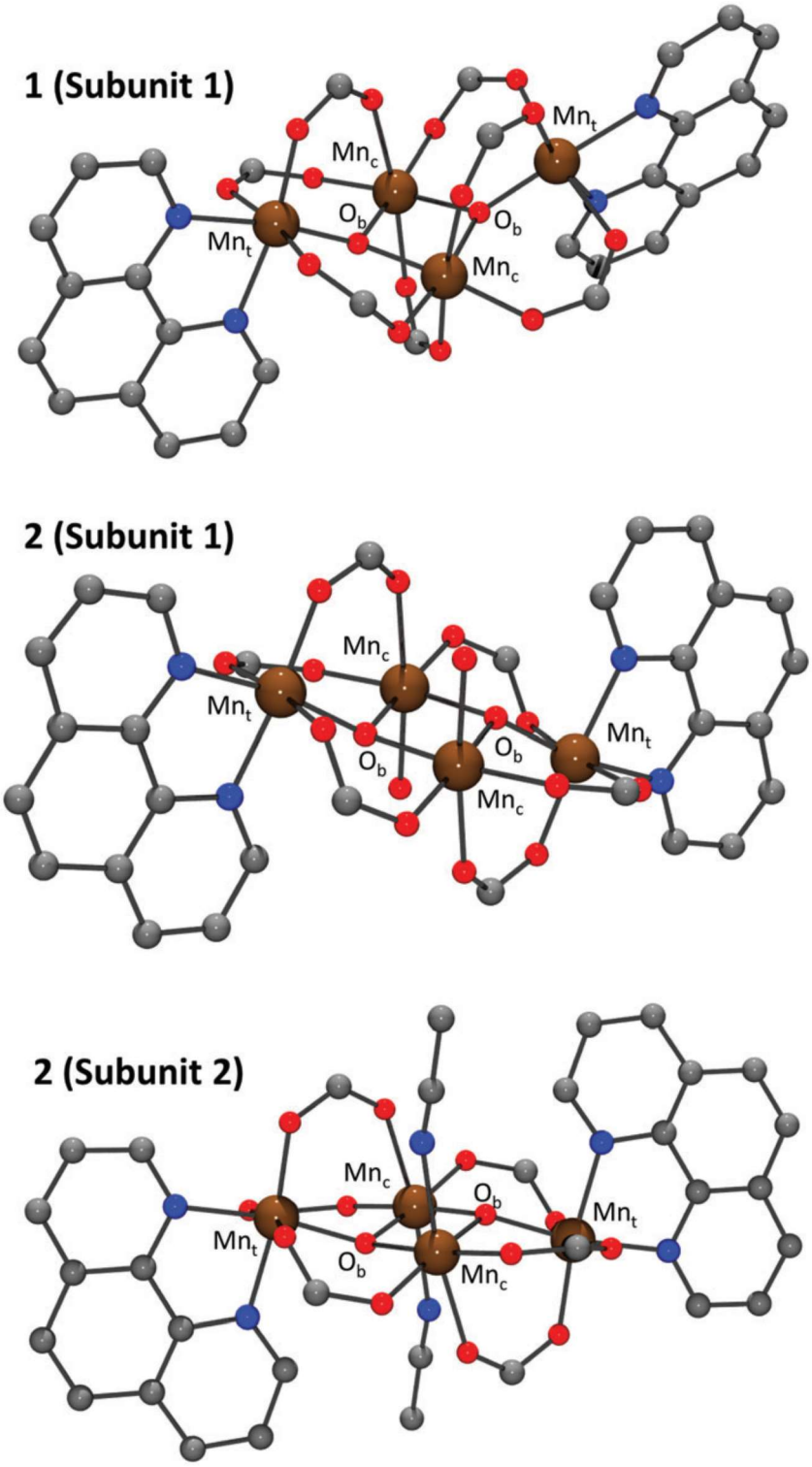

457

458

FIGURE 3

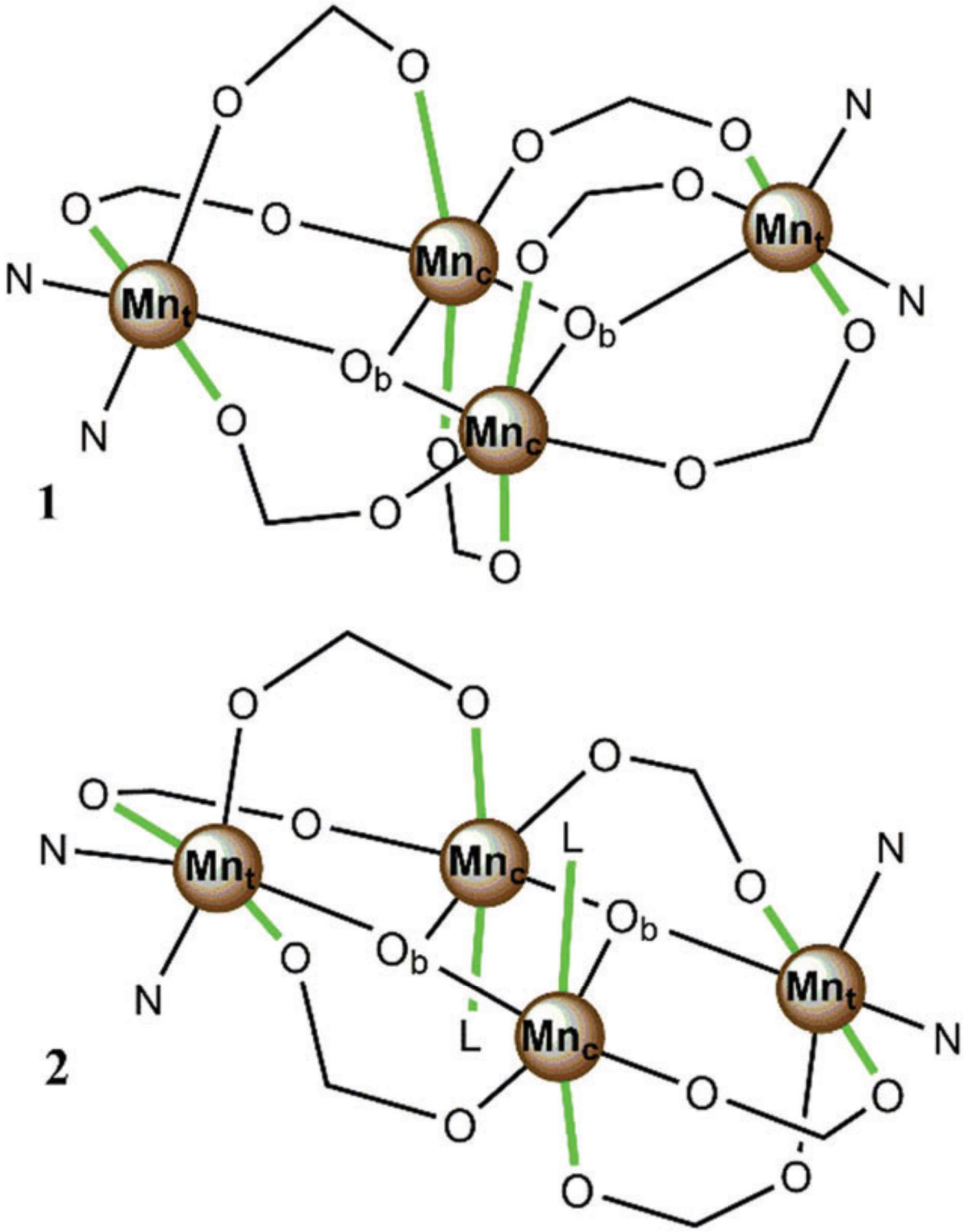

FIGURE 4

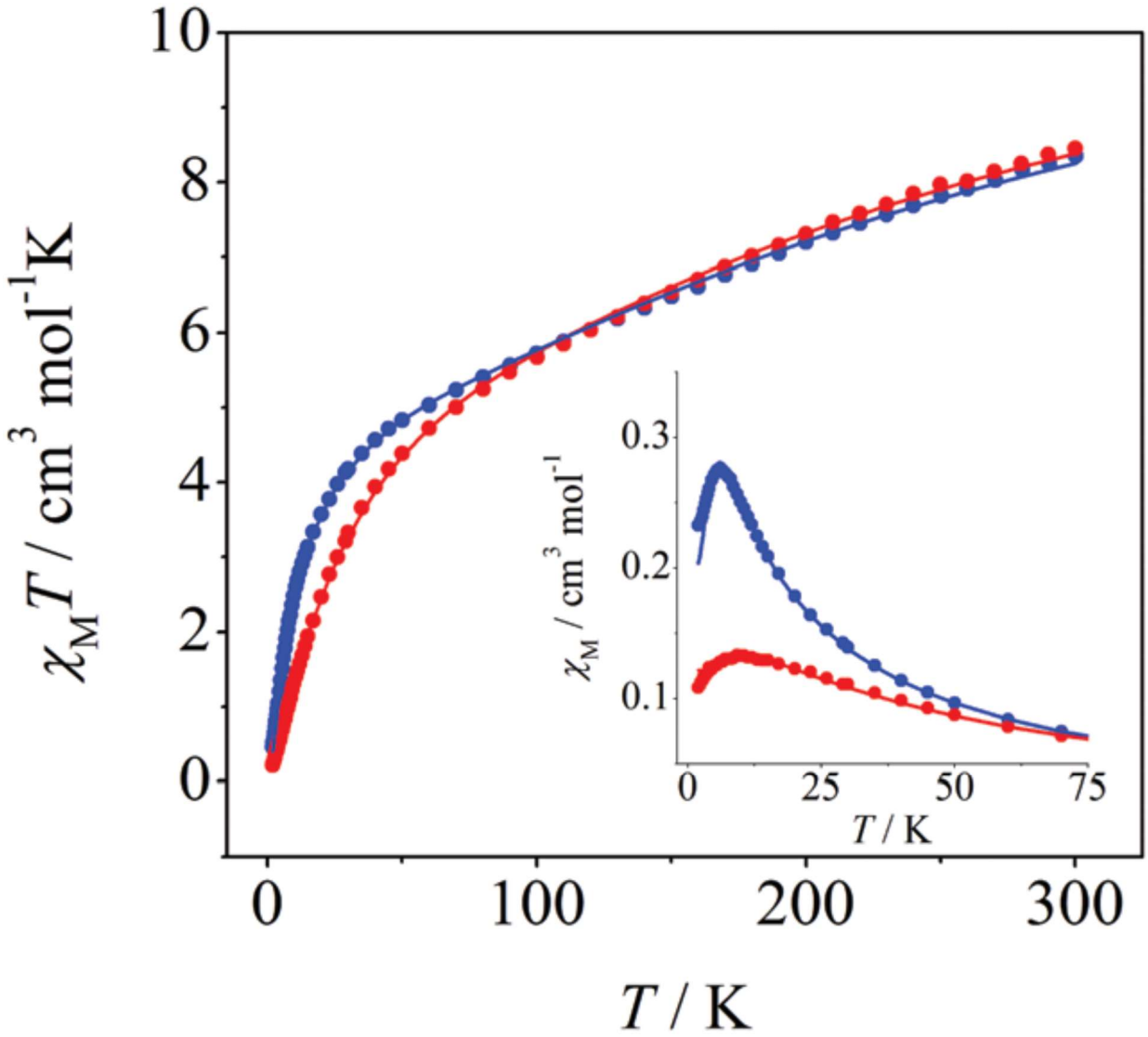
10
8
6
4
2
0
$\chi_M T$ / cm^3 mol^{-1}K
0
100
200
300
T / K
0.3
0.2
0.1
χ_M / cm^3 mol^{-1}
0
25
50
75
T / K

FIGURE 5

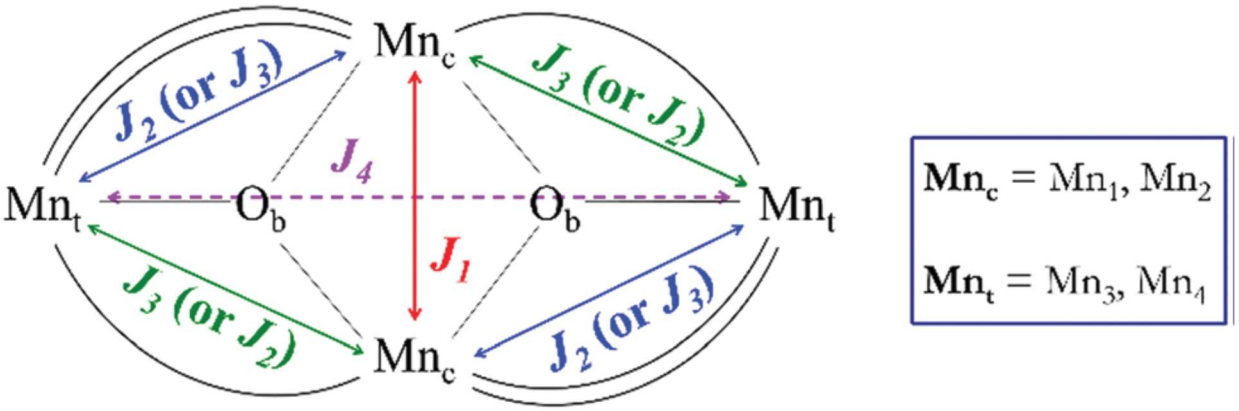
Mn$_c$
Mn$_c$
Mn$_t$
Mn$_t$
O$_b$
O$_b$
J_2 (or J_3)
J_3 (or J_2)
J_3 (or J_2)
J_2 (or J_3)
J_4
J_1
Mn$_c$ = Mn$_1$, Mn$_2$
Mn$_t$ = Mn$_3$, Mn$_4$

FIGURE 6

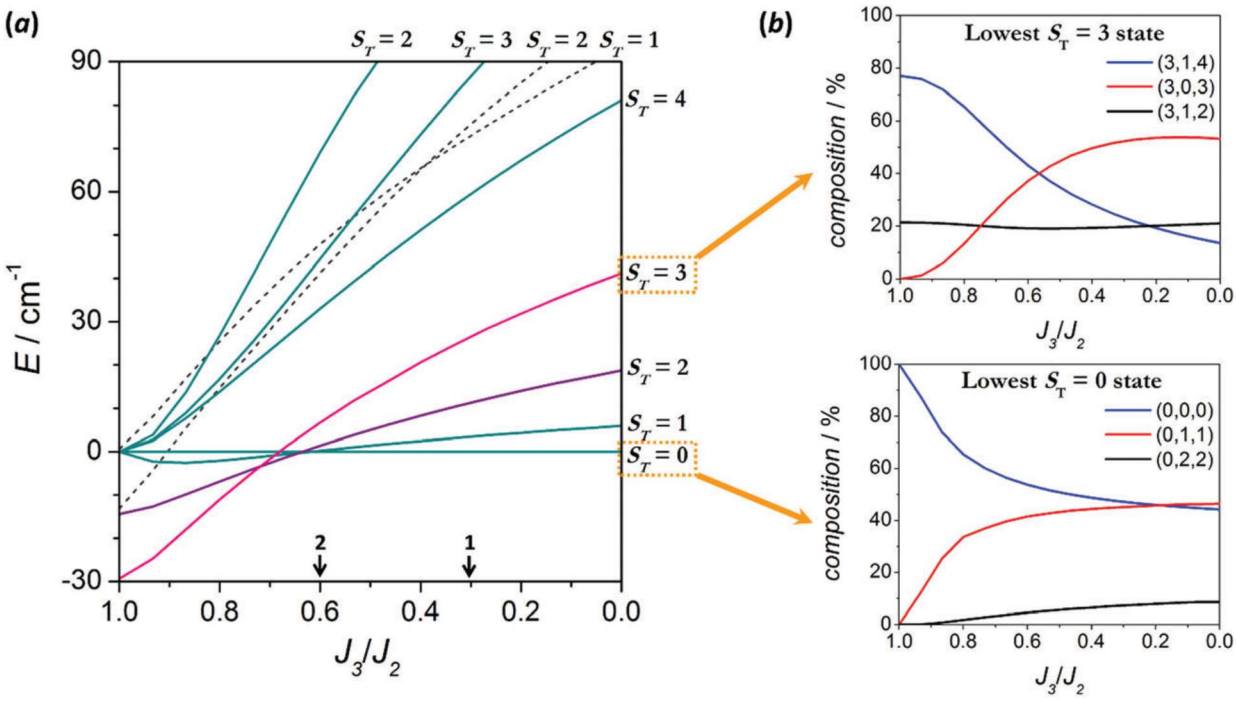
(a)
(b)
$S_T = 2$
$S_T = 3$
$S_T = 2$
$S_T = 1$
$S_T = 4$
$S_T = 3$
$S_T = 2$
$S_T = 1$
$S_T = 0$
E / cm^{-1}
J_3/J_2
2
1
Lowest $S_T = 3$ state
(3,1,4)
(3,0,3)
(3,1,2)
composition / %
Lowest $S_T = 0$ state
(0,0,0)
(0,1,1)
(0,2,2)

FIGURE 7